ICANS XIX,
19th meeting on Collaboration of Advanced Neutron Sources
March 8 – 12, 2010
Grindelwald, Switzerland

NEUTRON CROSS SECTIONS OF SOLID DEUTERIUM

J.R. GRANADA* and F. CANTARGI
Centro Atómico Bariloche and Instituto Balseiro
Comisión Nacional de Energía Atómica
8400 S.C. de Bariloche (RN), Argentina

ABSTRACT

We present calculations based on a new scattering kernel recently developed to describe the interaction of slow neutrons with solid Deuterium. The main characteristics of that system are contained in the model, including the lattice's density of states, the Young-Koppel quantum treatment of the rotations, and the internal molecular vibrations. The elastic processes involving coherent and incoherent contributions are fully described, as well as the spin-correlation effects. The results from the new model are compared with the best available experimental data, showing very good agreement, and predictions are made concerning the intensity and spectral characteristics of the neutron flux emerging from typical geometries.

* Also at CONICET, Argentina

1. Introduction

The fundamental properties of the hydrogen molecule, mostly in the liquid state, has been the subject of intense theoretical and experimental research. Purely quantum effects dominate the low-energy levels, as the total nuclear spin and the angular momentum become correlated due to the symmetry requirement on the total wave function of identical homonuclear diatomic molecules [1]. A complete description of the rotational motion in a gas of H_2 (and D_2) was produced by Young and Koppel [2], where the neutron cross sections for the *ortho* and *para* species were explicitly given. Although many models and calculational techniques were developed to describe the interaction of slow neutrons with liquid H_2 and D_2, the only prescription to calculate the cross section of solid hydrogen and deuterium was introduced by Bernnat *et al* [3], but spin correlation effects were not fully accounted for in that work.

In the last decade, the need to develop advanced moderators for ultracold neutron (UCN) physics studies has prompted an intense experimental effort to measure the neutron scattering properties of solid D_2 [4-9]. We have recently introduced a formalism aimed at providing the theoretical scheme to generate cross section data needed for the design and optimization of new and efficient UCN sources [10].

2. Basic equations

The Van Hove *scattering function* $S(\mathbf{Q},\omega)$ is directly related to the double-differential cross section:

$$\frac{d^2\sigma}{d\Omega d\omega} = \frac{k}{k_0} S(\mathbf{Q},\omega) \tag{1}$$

where $\mathbf{k}$, $\mathbf{k_0}$ are the scattered and initial neutron wave vectors, $\hbar\omega = \hbar^2(k_0^2 - k^2)/2m_n$ is the neutron energy loss, and $\hbar\mathbf{Q} = \hbar(\mathbf{k_0} - \mathbf{k})$ is the momentum transferred to the system in the process. For a molecular system [1]:

$$S(\mathbf{Q},\omega) = \frac{1}{2\pi\hbar}\int_{-\infty}^{\infty} dt e^{-i\omega t} \left\langle \sum_{l,l'}\sum_{\nu,\nu'} \overline{a^*_{l\nu} a_{l'\nu'}} \exp\{-i\mathbf{Q}.\mathbf{R}_{l\nu}(0)\}\exp\{i\mathbf{Q}.\mathbf{R}_{l'\nu'}(t)\} \right\rangle \tag{2}$$

where $\mathbf{R}_{l\nu}(t)$ denotes the position of the atom ν within the molecule l ,

$$\mathbf{R}_{l\nu}(t) = \mathbf{a}_l + \mathbf{b}_\nu(t) + \mathbf{u}_\nu(t) \tag{3}$$

and can be written as the sum of inter ($l \neq l'$)- and intra ($l = l'$)- molecular contributions (also referred to as the *outer* and *inner* terms, respectively). In Eq.(2) the brackets denote the so called *intermediate scattering function* $\chi(\mathbf{Q},t)$. In terms of the usual coherent, b_c^{ν} , and incoherent, b_i^{ν} , scattering lengths for nuclei ν, the scattering amplitudes $a_{l\nu}$ are

$$a_\nu = b_c^\nu + 2b_i^\nu (\mathbf{S}_\nu.\mathbf{s})\left[S_\nu(S_\nu+1)\right]^{-1/2} \tag{4}$$

where $\mathbf{S}_\nu$ and $\mathbf{s}$ are the spin operators for nuclei ν and the neutron, respectively.

The molecule's total wave-function must be symmetric under interchange of identical nuclei and then, if the total nuclear spin $\mathbf{S}$ is even the spatial nuclear wave function must be symmetric, and antisymmetric if $\mathbf{S}$ is odd, which leads, respectively, to the existence of the *ortho* states, with S = 0, 2 coupled to J = 0, 2, 4,…, and *para* states with S = 1 coupled to J = 1, 3, 5, …., where J denotes the molecule´s total angular momentum.

Leaving aside for the moment the consideration of vibrational modes, we can write the ´outer´ term of the intermediate scattering function as:

$$\begin{aligned}\chi^{out}(\mathbf{Q},t) &= \sum_{l\neq l'}\left\langle \exp\{-i\mathbf{Q}.\mathbf{a}_l(0)\}\exp\{i\mathbf{Q}.\mathbf{a}_{l'}(t)\}\right\rangle . \sum_{\nu,\nu'}\left\langle \overline{b^*_{l\nu}}\exp\{-i\mathbf{Q}.\mathbf{b}_{l\nu}(0)\}\overline{b_{l'\nu'}}\exp\{i\mathbf{Q}.\mathbf{b}_{l'\nu'}(t)\}\right\rangle \\ &\equiv I_d(\mathbf{Q},t)\ .\ u(\mathbf{Q})\end{aligned} \tag{5}$$

where

$$u(\mathbf{Q}) = |\Sigma_\nu \langle b_{l\nu}\exp\{i\mathbf{Q}.\mathbf{b}_\nu(0)\}\rangle|^2 = 4(b_c)^2 j_0^2(Qd/2) \tag{6}$$

which is the molecular structure factor with d (= 0.74 Å) being the interatomic distance, and j_0 the spherical Bessel function of order zero. The first factor in Eq.(5), $I_d(\mathbf{Q},t)$, represents the contribution due to molecular centers associated to *distinct* molecules.

The inner contribution to Eq.(2) is the Fourier transform of the corresponding intermediate scattering function:

$$\begin{aligned}\chi^{inner}(\mathbf{Q},t) &= \sum_{l}\left\langle \exp\{-i\mathbf{Q}.\mathbf{a}_l(0)\}\exp\{i\mathbf{Q}.\mathbf{a}_l(t)\}\right\rangle . \sum_{JJ'}\sum_{\pi\pi'} A_{\pi\pi'}(J) f_{\pi\pi'}(Q;J,J') e^{-i(\omega_J-\omega_{J'})t} \\ &\equiv I_s(\mathbf{Q},t)\ .\ v(\mathbf{Q},t)\end{aligned} \tag{7}$$

Here the first factor, $I_s(\mathbf{Q},t)$, is the *self* contribution of the molecular centers determined by the dynamics of the lattice in the case of solid systems. The second factor, $v(\mathbf{Q},t)$, contains all the complexity associated to the molecular rotations with definite parity for each (ortho,

para) molecular species. The coefficients $A_{\pi\pi'}$ and the functions $f_{\pi\pi'}$ in the last equation contain the specific values of the cross section values resulting from Eq.(4) for each rotational transition, and the corresponding rotational matrix elements, respectively [10].

As it is evident from the definitions of I_d (**Q**,t) and I_s (**Q**,t) from Eqs.(5) and (7),

$$I_d (\mathbf{Q},t) = I(\mathbf{Q},t) - I_s (\mathbf{Q},t) \tag{8}$$

and then the total intermediate scattering function is given by

$$\chi(\mathbf{Q},t) = 4\, b_c^2\, j_0^2\, (Qr/2)\, \{I (\mathbf{Q},t) - I_s (\mathbf{Q},t)\} + v(\mathbf{Q},t)\, .\, I_s (\mathbf{Q},t) \tag{9}$$

where $I(\mathbf{Q},t)$ now contains the contributions due to *all* molecular centers in the system.

Within the incoherent approximation for the inelastic term [1], $I(\mathbf{Q},t \neq 0) \cong I_s(\mathbf{Q},t\neq 0)$, and then

$$\chi^{inel}(\mathbf{Q},t) = v(\mathbf{Q},t)\, .\, I_s (\mathbf{Q},t)\, .\, \chi^{vib}(\mathbf{Q},t)\, . \tag{10}$$

While the elastic term, after a minor approximation neglecting small energy-dependent second order effects due to spin and structural correlations, can be written as [10]

$$\begin{aligned} \chi^{el}(\mathbf{Q},0) \;=\; & 4\, b_c^2\, j_0^2\, (Qr/2)\, |F(\mathbf{Q})|^2\; \chi^{vib}(\mathbf{Q},0) && \text{(Elastic Coherent)} \\ & + 2\,(1+\alpha)\, b_i^2\, \chi^{vib}(\mathbf{Q},0) && \text{(Elastic Incoherent)} \end{aligned} \tag{11}$$

with $\alpha = ¼$ for o-D_2, $-½$ for p-D_2, 0 for n-D_2, and $|F(\mathbf{Q},0)|$ the *hcp* lattice structure factor corresponding to the arrangement of molecular centers. Equations (10) and (11) are the basis of our new model for solid deuterium.

3. Results

The neutron scattering laws $S(\mathbf{Q},\omega)$, energy-transfer kernels $\sigma(E,E')$, and total cross sections $\sigma(E)$ for inelastic scattering in solid ortho- and para-deuterium were calculated using the code NJOY [11], which is based on a phonon expansion for the lattice motion and the Young-Koppel [2] formalism for the quantum rotational description. As part of the code´s input data, the lattice density of states (DOS) for solid deuterium derived by Schmidt *et al.*[12] was used. The elastic incoherent component produced by NJOY was modified in order to include spin correlation effects as indicated in Eq.(11). In our calculations we used the values $\sigma_c = 5.59$ b, $\sigma_i = 2.05$ b, for the bound atom coherent and incoherent cross sections respectively, and $\sigma_a = 0.0005$ b for the thermal neutron absorption cross section [13], as well as $\hbar\omega_r = 0.0074$ eV and $\hbar\omega_v = 0.371$ eV for the rotational and vibrational molecular energies.

The scattering function for solid deuterium at 5 K is displayed in Fig.1, in the form of $S(\alpha,\beta) = kT\, S(Q,\omega)$, where $\alpha = (\hbar^2 Q^2)/(2M.kT)$ and $\beta = \hbar\omega/kT$ with M being the molecular mass. We can observe in Fig.1a) the rather conventional behavior for ortho deuterium, where the inelastic processes are controlled by phonon interactions, for both up- ($\beta<0$) and down- ($\beta>0$) scattering, as revealed by the peaks observed at $\beta = \pm 11.5, \pm 21$, corresponding to the sharp maxima in the DOS at 0.005 eV and 0.009 eV [12], respectively. In Fig.1.b) we can see that the down-scattering side for para deuterium is again phonon-controlled, as it is essentially the case for up-scattering processes involving

very small momentum transfer. However, when the latter increases the up-scattering probability becomes much larger and of complex structure. The dominant feature is the peak at $\beta = -17.1$, corresponding to the rotational energy transferred to the neutron in the $J = 1 \rightarrow 0$ phononless transition, as the para- molecule converts into ortho.

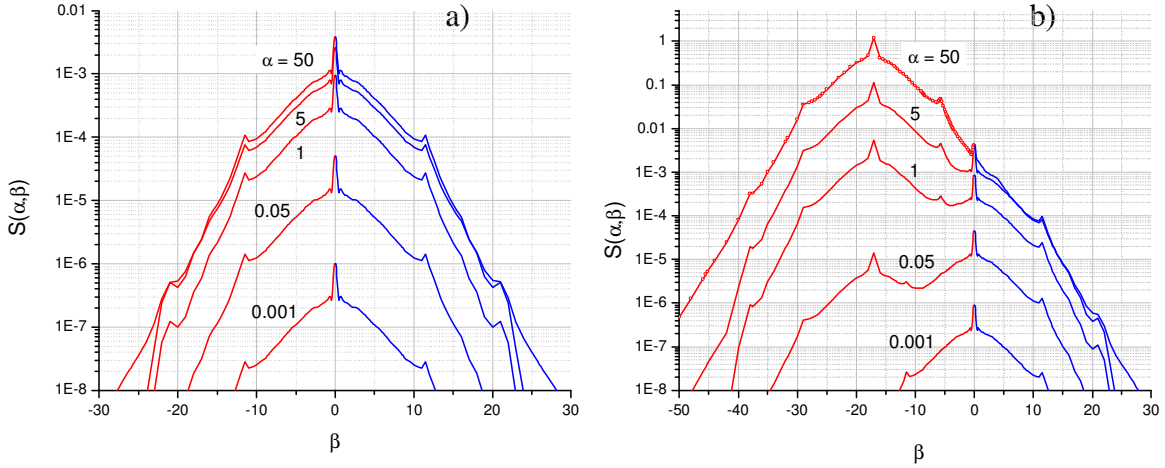

Fig.1: Scattering functions at low momentum transfer for solid D_2 at 5K, a) ortho, b) para.

Also, the scattering function for para-deuterium (Fig.1.b) shows a peak at $\beta = -5.7$ ($\hbar\omega = -0.0024$ eV), which is associated to a $J = 1 \rightarrow 0$ up-scattering transition ($\hbar\omega = -0.0074$ eV) coupled to phonon creation with a prominent energy of 0.005 eV, whereas the peak at $\beta = -28.8$ results from the same $J = 1 \rightarrow 0$ transition coupled to phonon annihilation ($\hbar\omega = -0.005$ eV). Finally, the peak observed at $\beta = -37.9$ ($\hbar\omega = -0.0164$ eV) is due to a similar coupling of rotational and phonon up-scattering processes, but in this case involving those with the large DOS at 0.009 eV. The processes referred to in this paragraph represent the first contributions to multiexcitation channels in the neutron interaction with s-D_2.

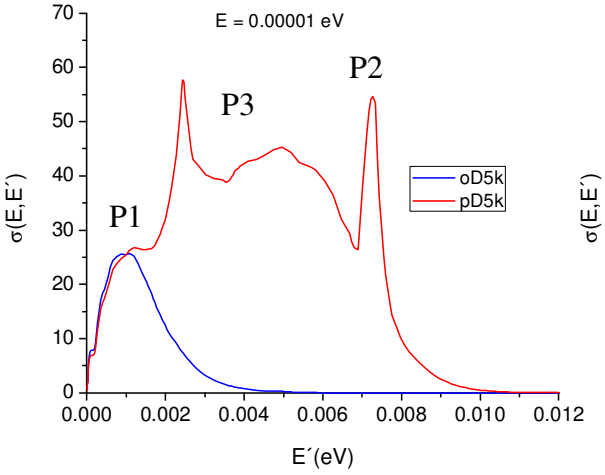

Fig.2: Energy-transfer kernels for pure ortho and para D_s at 5K and E=0.00001 eV.

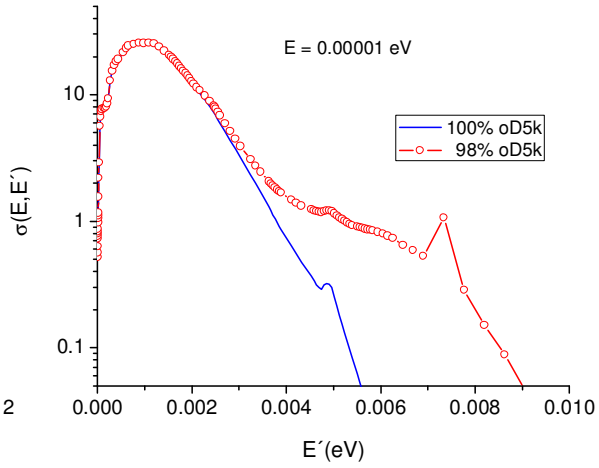

Fig.3: Energy-transfer kernels for 100% and 98% Ortho D_2 at 5K and E=0.00001 eV.

The processes just discussed are displayed in an even clearer manner through the behavior of the energy-transfer kernels shown in Fig.2, for an incident neutron energy E= 0.00001 eV. At 5K the solid ortho-D_2 has only low-energy phonons available to upscatter those incident neutrons through annihilation processes, P1, while a quite different picture corresponds to para-D_2. Besides the existence of the same processes P1, we identify J = 1→0 phononless transitions (P2), and the J = 1→0 transition coupled to phonon creation with a range of energies including the large DOS acoustic excitations at 0.005 eV (P3). The effect of a 2% para contamination is shown in Fig.3, where the energy-transfer kernel displays the increased upscattering cross section under the same conditions.

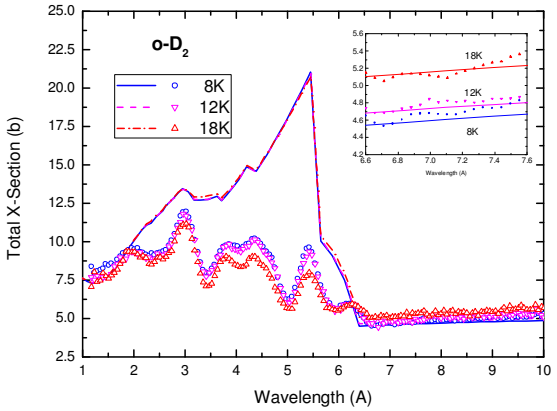

Fig.4: Calculated total cross section of solid o-D_2 at a few temperatures, compared with experimental data from [7,14]. See text for details.

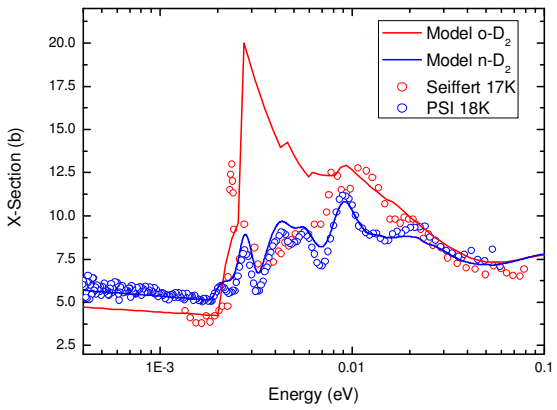

Fig.5: Calculated total cross sections of ortho- and normal-deuterium at 18 K, compared with the experimental data from ref. [7] and [15] around 18K.

The calculated total cross section of ortho-deuterium is shown in Fig.4, compared with experimental data from Refs.[7] and [14] for a few temperatures over the thermal neutron wavelength range. The large elastic coherent contribution due to the *hcp* structure factor dominates the cross section at those energies, and the disagreement with the measured points is a clear indication of the lack of perfect polycrystallinity in the samples.

However, a very nice agreement between both sets is observed beyond the first Bragg peak, a region dominated by total inelastic and incoherent (including spin correlation effects) elastic components of the total cross section (see inset in fig.4).

We have incorporated the specific structure observed in the PSI measurements into the elastic coherent cross section, instead of that for the ideal polycrystalline solid. The result is displayed in fig.5, where we compare our calculations for ortho and normal solid D_2 with experimental data from Refs. [7] and [15].

At about 18K the inelastic cross section for ortho and para deuterium are very similar, and therefore the differences observed in the cross sections of ortho- and normal-deuterium at energies below the onset of coherent effects are purely due to spin correlation effects on the elastic incoherent contribution.

4. Conclusions

A new scattering kernel to describe the interaction of slow neutrons with solid Deuterium has been developed. The main characteristics of this molecular solid are contained in the formalism, including dynamical aspects related to:

- the lattice's density of states,
- the Young-Koppel quantum treatment of the rotational motion, and
- the internal molecular vibrations.

The elastic processes involving coherent and incoherent contributions are also fully described, as well as the spin-correlation effects caused by the coupling of intrinsic and rotational angular momenta.

The scattering functions and cross sections for both *ortho-* and *para-* Deuterium have been evaluated for temperatures ranging from the freezing point (18.7 K) down to 5 K.

The new model has been compared with the best available experimental data, showing a highly satisfactory agreement.

5. Acknowledgements

It is a pleasure to acknowledge very interesting discussions with K. Kirch and M. Kasprzak at PSI concerning the measurements on solid deuterium performed at that Institute during the last few years. This work was partially supported by grant PICT 52963 from ANPCyT (Argentina) and IAEA RC Nº 14161 funds.

6. References

1. S.W. Lovesey, *Theory of Neutron Scattering from Condensed Matter* (Clarendon Press, Oxford, 1984).
2. J.A. Young and J.U. Koppel, *Phys.Rev.* **135** (1964) A603; J.U. Koppel and J.A. Young, *Nukleonika* **8**(1966) 40.
3. W.Bernnat, J. Keinert and M. Mattes, in *Advanced Cold Moderators, Proceedings of the 6th. Internat. Workshop on Advanced Cold Moderators*, ISSN 1433-5506, edited by H. Conrad, (FZ Julich, Germany, 2002) p.9.
4. A. Serebrov *et al.*, *Nucl.Instr.Meth.* **A440** (2000) 658.
5. C.L. Morris *et al.*, *Phys.Rev.Lett.* **89** (2002) 272501.
6. A. Saunder *et al., Phys.Lett.* **B 593** (2004) 55.
7. F. Atchison *et al.*, *Phys.Rev.Lett.* **95** (2005) 182502-1: *ibid* **99** (2007) 262502-1.
8. I. Altarev *et al., Eur.Phys.J.* **A 37** (2008) 9.
9. A. Frei *et al.*, *Phys.Rev.* **B80** (2009) 064301-1: E. Gutsmiedl *et al., Nucl.Instr.Meth.* **A611** (2009) 256.
10. J.R. Granada, *EPL.* **86** (2009) 66007.
11. R.E. MacFarlane and D.W. Muir, LANL Report LA-12740-M (1994).
12. J.W. Schmidt *et al.*, *Phys.Rev.***B 30** (1984) 6308.

13. *Neutron News* **3** (1992) 29.
14. M. Kasprzak, *PhD Thesis*, University of Vienna (2008).
15 W.D. Seiffert W, Report EUR 4455d (1970).